Jordan Journal of Civil Engineering, Volume **19**, No. **2**, **2025**
DOI: https://doi.org/10.14525/JJCE.v19i2.01

Jordan Journal of Civil Engineering

Journal homepage: https://jjce.just.edu.jo

Durability and Microstructural Analysis of Mortar Incorporating Glass Powder and Copper Slag

Shruti Bhargava [1),2)], ***Kishan Lal Jain*** [3)*], ***P.V. Ramana*** [4)], ***Dinesh Kumar Sharma*** [5)]

[1)] *Research Scholar, Department of Civil Engineering, Malaviya National Institute of Technology, Jaipur-302017. E-Mail: 2023rce9004@mnit.ac.in*
[2)] *Assistant Professor, Arya College of Engineering, Jaipur, Rajasthan-302022, India.*
[3*)] *Associate Professor, Department of Civil Engineering, Swami Keshvanand Institute of Technology, Management & Gramothan, Jaipur, Rajasthan-302017, India. *Corresponding Author. E-Mail: kishan.jain@skit.ac.in*
[4)] *Associate Professor, Department of Civil Engineering, Malaviya National Institute of Technology, Jaipur-302017. E-Mail: pvramana.ce@mnit.ac.in*
[5)] *Professor, Department of Civil Engineering, Swami Keshvanand Institute of Technology, Management & Gramothan, Jaipur, Rajasthan-302017, India. E-Mail: dks@skit.ac.in*

ARTICLE INFO

Article History:
Received: 18/10/2024
Accepted: 8/2/2025

ABSTRACT

Untreated solid waste presents significant environmental challenges, particularly in areas surrounding industrial activities. This study investigates a sustainable solution through the utilization of industrial by-products—copper slag from the iron industry and waste glass powder from soda-lime glass bottles—in mortar production. Mortar mixtures were prepared with partial replacements: cement was replaced with glass powder (GP) at 5%, 10%, 15%, 20%, and 25%, while fine aggregate was replaced with copper slag (CS) at 0%, 10%, 20%, 30%, 40%, and 50%, maintaining a cement-to-fine aggregate ratio of 1:4. Key properties were assessed through comprehensive laboratory tests, including compressive strength; shear bond strength, drying shrinkage, flowability, and water absorption. Microstructural properties were analyzed using scanning electron microscopy (SEM), X-ray diffraction (XRD), Thermogravimetric analysis (TGA), and Fourier-transform infrared spectroscopy (FTIR). Results indicate an initial decrease in compressive strength at lower replacement levels, followed by a significant improvement that surpasses the reference mortar. Optimal performance was achieved with 20% copper slag as sand and 10% glass powder as cement, improving multiple properties despite variations in drying shrinkage and shear bond strength. This research underscores the potential of glass powder and copper slag to enhance the performance and sustainability of construction materials, providing an effective pathway for waste valorization in the construction industry.

Keywords: Glass powder, Copper slag, Shear bond strength, Drying shrinkage, Water absorption, Microstructure.

INTRODUCTION

The increasing adoption of industrial waste materials across various sectors reflects a growing commitment to environmental conservation, pollution reduction, and resource sustainability. As global waste production surges, governments are actively implementing policies and funding research initiatives to promote the utilization of waste materials. Industrial by-products, such as slag (Mobasher et al., 1996), fly ash (Hwang et al., 1998), iron slag (Jain et al., 2022), waste glass (Degirmenci & Yilmaz, 2011), and plastics (Duan et al.,

2020), once relegated to landfills, are now being repurposed in construction applications, including road pavements, concrete production, and metal refining (Abukersh & Fairfield, 2011). India produces a large amount of industrial waste each year, creating considerable potential for commercialization and recycling. In the fiscal year 2022, the country generated more than 62 million tons of waste, of which 43 million tons were collected, and 12 million tons were treated prior to disposal. Among these materials, copper slag is particularly valuable due to its abundance as a by-product of metal refining. The growing production of metals has resulted in significant slag volumes, necessitating effective management strategies. As the construction sector grapples with resource depletion and rising demand for building materials, the shift towards secondary materials is becoming increasingly vital (Driouich et al., 2020). Asia, notably, is a leading producer of copper slag, with major smelters located in India, such as Hindalco, Sterlite Copper, and Hindustan Copper, Ltd. (Batis et al., 2015). Research into the use of copper slag in construction dates back to the 1980s, gaining traction, particularly in Singapore. The properties of copper slag vary based on cooling methods; air-cooled slag, for instance, exhibits superior pozzolanic activity due to its denser structure. Investigations have shown that replacing fine aggregate with copper slag can enhance the compressive and flexural strengths of mortar (Bilir et al., 2015). Studies indicated that up to 50% replacement can lead to significant strength improvements (Aouan et al., 2021). Additionally, the incorporation of calcined waste aggregates has demonstrated enhanced durability and reduced weight loss in mortars (Borhan & Mohamed, 2022). The use of waste granite powder as a fine aggregate has also been linked to improvements in compressive strength and microstructural properties (Gupta & Vyas, 2018). Further research has highlighted the efficacy of various alternative materials, such as fly ash, bottom ash, and metakaolin, as replacements in mortar formulations, optimizing performance and sustainability (Kallel et al., 2021). To address the depletion of natural resources, studies are increasingly focusing on substituting fine aggregates with granulated lead smelter slag, glass sand, and copper slag (Srinivasreddy et al., 2022). Earlier research has investigated the use of copper slag (CS) as a partial substitute for sand and coarse aggregates in cement-based composites. A comprehensive review of 96 studies revealed that CS enhances the physical properties of these composites, notably improving workability in the fresh state and boosting compressive strength in the hardened state, especially when CS content reaches up to 70%. (Cezar Augusto Casagrande et al., 2023). Kaolin clays, recognized for their pozzolanic properties, present additional potential, although their usage is often limited to low proportions due to reactivity concerns (Kou & Poon, 2020). The development of ternary blended binder systems, combining raw kaolin with reactive materials, shows promise in enhancing performance (Saranya et al., 2021). Research demonstrated that concrete mixtures with 30% glass powder and polypropylene fibers yield increased tensile strength (Sivasakthi, 2021). Moreover, substituting 15% to 45% of cement with glass powder has improved compressive strength while reducing porosity (Saiz Martinez et al., 2017). Cement binders with 15% glass powder exhibit significant pozzolanic properties, enhancing density and strength (Bilir, 2010). Ternary blended geopolymers have garnered attention due to their superior properties compared to mono- and binary blends. For instance, incorporating 10% fly ash into a mix of 70% slag and 30% metakaolin resulted in a remarkable increase in compressive strength (Ramadoss & Sundararajan, 2014). Similarly, a life cycle assessment revealed that ternary blends containing recycled construction materials exhibit lower embodied energy and CO_2 emissions, highlighting their sustainability benefits (Xu et al., 2021).

In summary, existing literature underscores the significant potential of copper slag as a fine aggregate replacement and glass powder as a cement alternative in mortar applications. These materials contribute to improved performance through their pozzolanic activity and favorable physical properties, promoting sustainability in construction by recycling industrial by-products. This study aims to expand on this foundation by conducting a comprehensive evaluation of mortar performance with copper slag and glass powder. By simulating real-world conditions, the research will assess key engineering properties, including compressive strength, shear bond strength, drying shrinkage, and durability factors, ultimately providing insights into optimal proportions for enhanced sustainability in construction materials.

MATERIALS AND MIX CALCULATIONS

The fine aggregate utilized in this research comprises Zone II (IS 383, 2016) Banas River sand. To replicate authentic field conditions during experimentation, IS sieves were intentionally omitted during the mix preparation process. Instead, only those materials that are typically screened on field sites using locally available sieves, commonly referred to as "tatti," "zarri," "jaali," and the like, were employed. The index properties of the fine aggregate are presented in Table 1. Copper slag was chosen as a replacement for the fine aggregate based on weight. Glass powder, derived from recycled soda-lime glass bottles, was finely ground and sieved through a 90-micron mesh, ensuring uniform particle size distribution for enhanced pozzolanic activity. Ordinary Portland cement, specifically of 43 grade (IS 8112, 2012), was consistently employed throughout the experimental investigation. The cement's characteristics were assessed in the laboratory, and the test results are presented in Table 1. Figure (1) represents the particle size distribution curves for river sand and copper slag. Microstructural analysis using Scanning Electron Microscopy (SEM) revealed significant textural differences between river sand and copper slag. As shown in Figure (2), SEM micrographs highlight the rough and irregular surface texture of slag particles, which is anticipated to improve mechanical interlocking within the concrete matrix. In contrast, river sand displayed a smoother surface. The chemical compositions of cement, river sand, CS and GP were analyzed through X-ray Diffraction (XRD) analysis, presented in Table 2. Higher proportions of quartz and alumina were identified in both sand and copper slag, as detailed in Figures 3(a) and 3(b). These findings suggest that copper slag offers a comparable mineral profile to river sand, supporting its suitability as a sand replacement in concrete.

Table 1. Index properties of cement, river sand, copper slag and glass powder

Property/ Parameter	Fineness Modulus	Specific Gravity	Water Absorption (%)	Bulk Density (g/cc)	Bulking of Fine Aggregate/ Zone	Soundness	Fineness	Consistency	Setting Time
River Sand	2.82	2.66	15.4	1.585	20.20/ II	-	-	-	-
Copper Slag	2.75	2.71	12.3	1.589	16.25/ II	-	-	-	-
Glass Powder	0.91	2.53	0.80	2.586	-	-	-	-	-
Cement	-	3.07	-	-	-	2mm	5%	29%	5hr.

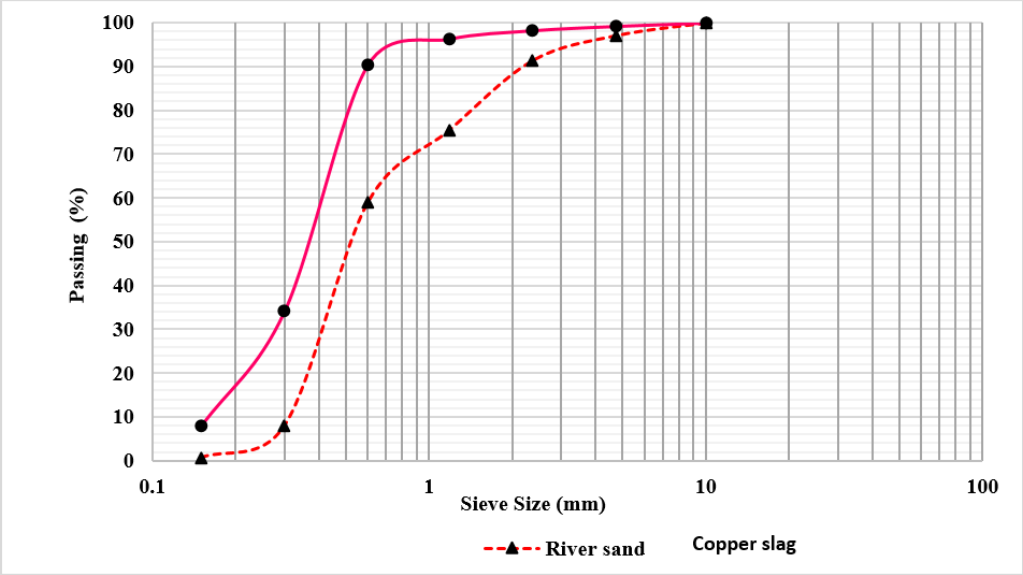

Figure (1): Particle size distribution for natural river sand and copper slag

Table 2. Chemical composition of concrete constitutes

Composition (%)	CaO	SiO_2	Al_2O_3	Fe_2O_3	MgO	SO_3	MnO	Na_2O	K_2O	TiO_2	P_2O_5	H_2O
Cement	64.9	21.00	4.2	2.3	1.5	1.7	-	0.33	0.45	-	-	-
Sand	3.45	72.23	10.75	3.60	1.29	-	0.05	2.30	1.91	0.43	0.10	-
CS	2.10	71.15	13.80	3.37	0.85	-	0.15	3.35	4.15	0.33	0.23	0.80
GP	9.8	73.00	0.35	0.28	3.08	-	-	13.79	0.16	-	-	-

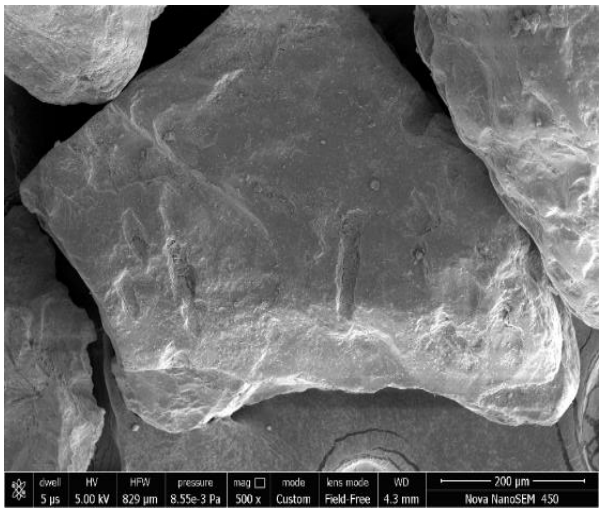

Figure (2): (a) SEM micrograph of river sand

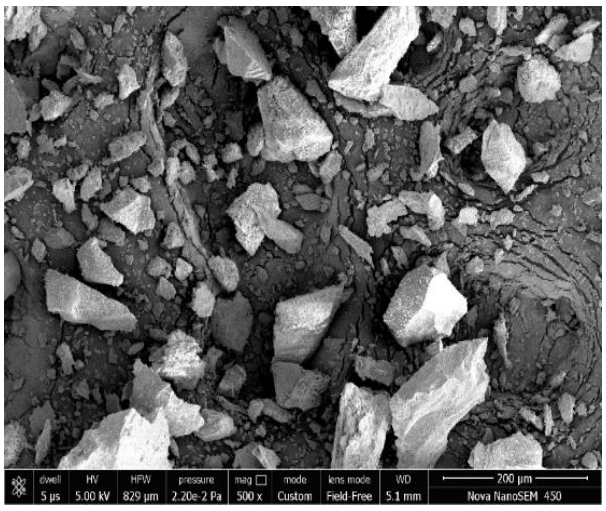

(b) SEM micrograph of copper slag

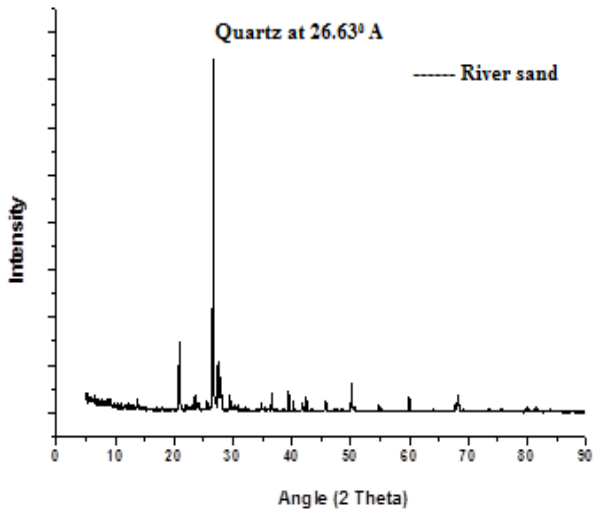

Figure (3): (a) XRD pattern for river sand

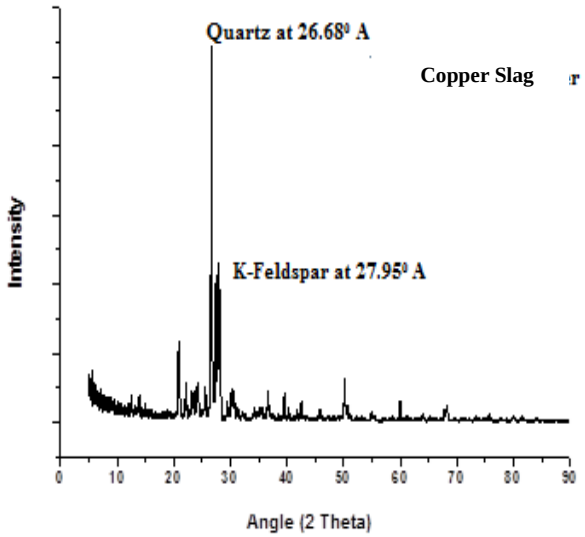

(b) XRD pattern for copper slag

Mix Calculations

This study established the cement-to-fine aggregate ratio for masonry mortar as 1:4 by weight. Applying the flow table test and following ASTM C1437-15 guidelines, an optimum and suitable water-cement ratio was determined for each replacement percentage. This approach aimed to achieve mortar with a flow value (representing workability) falling within the range of 105% to 115%, as determined through the flow table test. During the mixing process, manual methods were employed, and the water-cement ratio was calculated and maintained consistently across all mixtures. The

composition of constituents for every 100 grams of the mix is shown in Table 3.

Table 3. Mix design (per 100 grams)

Percentage Replacement or %	Cement	Glass Powder	Fine Aggregate or Copper S/ag		Water	Water-Binder Ratio
			Fine Aggregate	Copper Slag		
CM00	16.72	0	66.89	0	16.39	0.92
CG0510	17.01	0.85	61.22	6.8	14.97	0.88
CG1020	17.08	1.70	54.65	13.66	14.60	0.86
CG1530	17.25	2.58	47.89	20.36	16.39	0.82
CG2040	17.55	3.51	48.22	27.28	14.97	0.80
CG2550	18.15	4.53	48.65	34.32	14.60	0.79

CM00 = Control mix.

CG = Copper slag and Glass powder GP=5,10,15,20, and 25% CS=10,20,30,40, and 50% (GP/CS; 5/10, 10/20,15/30, 20/40 and 25/50).

METHODOLOGY

Flow Table Test

This test was conducted following IS 4031-1988, Part-7 to determine the optimal water content. Multiple trials were performed for different replacement percentages, aiming for a flow value between 105% and 115% to ensure proper workability. A frustum mold (top Ø 70 mm, bottom Ø 100 mm, height 50 mm) was used on a flow table. The mold was lubricated, centrally placed, and filled in three layers, with each layer tamped 20 times. After removing the mold, the table was subjected to 25 automated drops. All mortar mixes were prepared manually for the test, as shows in Figure (4).

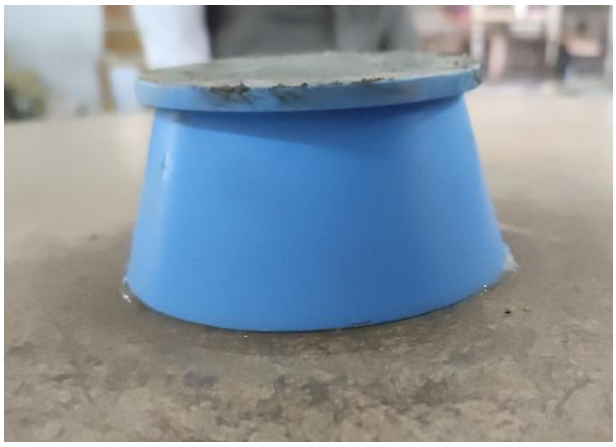

Figure (4): (a) Frustum mortar mold (b) Flow table in preparation

Drying Shrinkage

This test followed ASTM C1148-92a. Shrinkage beams (25 mm × 25 mm × 282 mm) were cast in molds, which were disassembled for specimen removal and reused. A scale with 0.001 mm precision, calibrated daily with a calibration rod, was used. The scale module was detachable and mounted on the length comparator. Mortar was mixed manually, compacted using a tamping rod and vibrating table, and smoothed with a trowel. Excessive vibration was avoided to prevent bleeding. Specimens were de-molded after 3 days of jute-bag curing and submerged in water for 4 more days. Observations were recorded at 1 day and 27 days, slightly differing from the standard (1 day and 28 days).

Figure (5) shows the shrinkage beam with length comparator and curing shrinkage beams.

Figure (5): (a) Shrinkage beam mould **(b) Length comparator**

(c) Curing shrinkage beams

Compressive Strength

Compressive strength testing followed IS 4031-1988, Part-6. Cube molds (50-mm sides) were filled in three layers, with each layer tamped 25 times. A vibrating table was used to remove air bubbles and ensure a smooth finish without bleeding. The openable molds were greased, reassembled, and removed after one day. Specimens were then cured by submersion for 27 days. Compressive strength tests were conducted on a consulting laboratory's machine with a slow loading rate. The rate of loading applied was $2N/mm^2$ to $6N/mm^2$ for each specimen. Three samples per replacement percentage were tested at 28 days. Figure (6) shows the mortar cubes and curing tank.

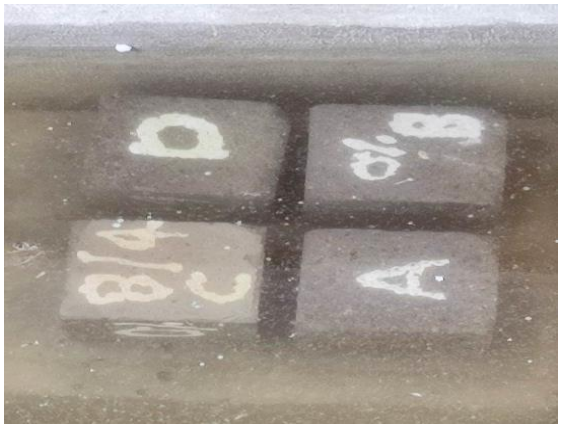

Figure (6): (a) Mortar 50-mm cube mould **(b) Mortar specimen in curing tank**

Shear Bond Strength Test (Masonry Triplet Test)

In this study's brick bond strength investigation, the triple masonry test was employed. The triple masonry test, following BS 1015-12:2000, was used to assess brick bond strength. Mortar was mixed manually. The joints were compacted using a trowel and secured with wooden pegs to prevent leakage during analysis. Two samples were prepared for each replacement percentage, as shown in Figure (7). Membrane curing was applied using jute bags. Samples were tested on the same machine at a slow loading rate, with joint strength recorded at failure. Failure patterns were also observed for analysis.

Figure (7): (a) Brick spacing

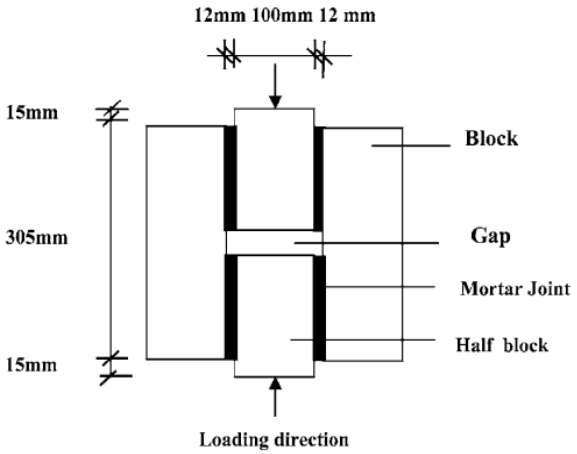

(b) Arrangement for masonry triplet test

Water Absorption

This test was conducted following ASTM C642-13 standard. It involved monitoring an increase in mass after immersion. The test cubes were prepared using a 50-mm mold for mortar. The samples were subjected to 24 hours of oven drying 28 days after their preparation, followed by complete submersion in water for at least 48 hours and then another round of oven drying. The temperature was carefully controlled within the 100 to 110 degrees Celsius range. Mortar cubes were cast for each replacement level, de-molded one day after casting, and submerged for 27 days before testing, as shown in Figure (8). A vibrating table was used during the casting process. Efforts were made to maintain temperature during the test. However, it is worth noting that the samples with a 10% replacement of Glass Powder (GP) and Copper Slag (CS) were subjected to elevated temperatures without showing any adverse effects.

Figure (8): (a) Weighing cube after 48 hours of immersion (b) Oven drying the samples at 110°C

RESULTS AND DISCUSSION

Compressive Strength

The test results indicate in Figure (9), that the incorporation of GP and CS in the mortar mix leads to an increase in density. Among the tested samples, the mortar mix with a (10% GP, 20% CS) replacement exhibited the highest average compressive strength, followed by the reference mortar mix. The reference mortar mix, without any GP and CS replacement, exhibited a lower average compressive strength compared to the (15% GP, 30% CS) mix. The superior performance of these mixes can be attributed to the larger surface area of GP and CS particles, which increases water absorption. This reduces the water-binder ratio, ultimately leading to enhanced compressive strength (Ling et al. ,2020). The 25% GP and 50% CS copper slag replacement mortar mix showed the lowest average compressive strength among the tested samples. This reduction in strength can be attributed to the inability to meet the designed water requirements at higher replacement levels, resulting in unhydrated binder particles. Consequently, this limits the formation of calcium silicate hydrate (CSH) gel, which is crucial for the development of compressive strength (Duan et al., 2020). The detailed compressive strength results are presented in Table4.

Table 4. Results of compressive strength test on mortar mixes

Sample	Compressive Strength (MPa)	Density gm/cm^3	Remark	Average
CM00(1)	8.424	2.174	Reference mortar, 0%	8.85 N/mm^2
CM00(2)	9.54	2.157	Reference mortar, 0%	
CM00(3)	8.545	2.136	Reference mortar, 0%	
CG510 (1)	8.472	2.228	10 % copper slag, FS Replacement	7.48 N/mm^2
CG510 (2)	6.504	2.202	10 % copper slag, GP Replacement	
CG510 (3)	7.468	2.219	10 % copper slag, GP Replacement	
CG1020 (1)	9.5	2.289	10 % copper slag, GP Replacement	8.90 N/mm^2
CG1020 (2)	8.66	2.283	10 % copper slag, GP Replacement	
CG1020 (3)	8.59	2.312	10 % copper slag, GP Replacement	
CG1530 (1)	8.251	2.174	10 % copper slag, GP Replacement	8.57 N/mm^2
CG1530 (2)	9.23	2.283	10 % copper slag, GP Replacement	
CG1530 (3)	8.22	2.312	10 % copper slag, GP Replacement	
CG2040 (1)	8.10	2.302	10 % copper slag, GP Replacement	7.08 N/mm^2
CG2040 (2)	6.23	2.283	10 % copper slag, GP Replacement	
CG2040 (3)	7.02	2.325	10 % copper slag, GP Replacement	
CG2550 (1)	7.10	2.189	10 % copper slag, GP Replacement	6.40 N/mm^2
CG2550 (2)	6.10	2.183	10 % copper slag, GP Replacement	
CG2550 (3)	6.02	2.312	10 % copper slag, GP Replacement	

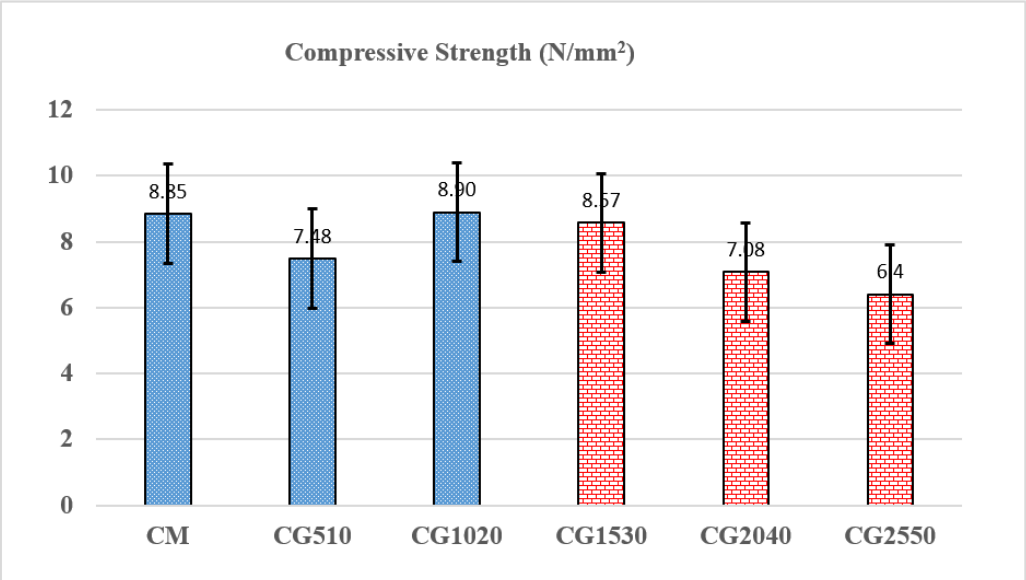

Figure (9): Test results of compressive strength

Drying Shrinkage of Mortar

The results show in Figure (10) the shrinkage of mortar beams with varying levels of copper slag (CS) and glass powder (GP) replacement, observed over 27 days. Lower replacement levels of glass powder and copper slag (10% GP, 20% CS) significantly reduce shrinkage, while higher replacements (25% GP, 50% CS) result in increased shrinkage, potentially due to reduced cohesion and increased porosity in the mortar matrix. Optimal performance seems to occur at moderate replacement levels which improve shrinkage behavior compared to the control mix (Ramadoss & Sundararajan, 2014). The mortar mix CG2550% exhibited the highest shrinkage over a 27-day period, indicating a significant influence on the mix design. An increasing trend in drying shrinkage was observed with higher proportions of copper slag in the mortar mix. This may be attributed to the reduced cohesion and higher porosity within the mortar matrix. Furthermore, the increased proportions of GP and CS could affect the microstructure of the mortar, leading to less effective hydration and weaker particle bonding, which in turn results in higher shrinkage (Abukersh & Fairfield, 2011; Sivasakthi et al., 2021).

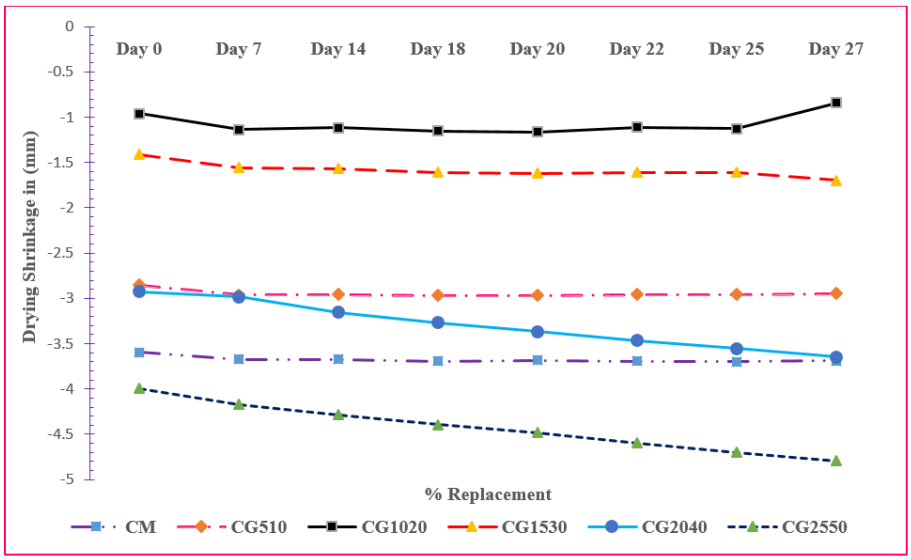

Figure (10): Graph for visualizing shrinkage behavior relative to each specimen

Water Absorption Ratio

Figure (11) shows the test results of water absorption of control and blended mortar mixes. The CG1020 mix (10% GP, 20% CS) demonstrates the lowest water absorption at 6.87%, indicating improved density and reduced porosity. CG1530 (15% GP, 30% CS) follows closely with 6.49%, suggesting that these replacement levels enhance the mortar's impermeability. Good mortar mixes absorb water below 10 percent by mass. The scale or degree of water absorbed is influenced by the materials used, and the duration of exposure affects the strength of the mortar (Saranya et al., 2021). The CG2040 mix (20% GP, 40% CS) shows a water absorption of 7.66%, indicating that while performance is still acceptable, it is higher than those of CG1020 and CG1530, possibly due to increased porosity from the higher slag content. CG2550 (25% GP, 50% CS) has a water absorption rate of 7.87%, suggesting that excessive replacement may lead to increased porosity and, therefore, to higher water absorption. Notably, the dry weight after drying is anomalously low (2 g), which may indicate an experimental error. The replacement of traditional materials with GP and CS appears to have beneficial effects on water absorption up to a certain level. The optimal ranges seem to be around 10% GP and 20% CS, where water absorption is minimized. The increasing trend in Table 5 of water absorption at higher replacement levels indicates potential limitations of these materials when used in excess (Kallel et al., 2021).

Table 5. Observed behavior of mortar specimens in context of water absorption

Sample replacement %	Dry weight after curing (24 hours oven dry) in gram	Wet weight after 48 hours of submersion in gram	Dry weight after drying 24 hours in oven in gram	Water Absorption
CM00	258	281	259	8.49%
CG510	254	276	254	8.66%
CG1020	262	280	262	6.87%
CG1530	264	283	246	6.49%
CG2040	268	275	220	7.66%
CG2550	270	285	221	7.87%

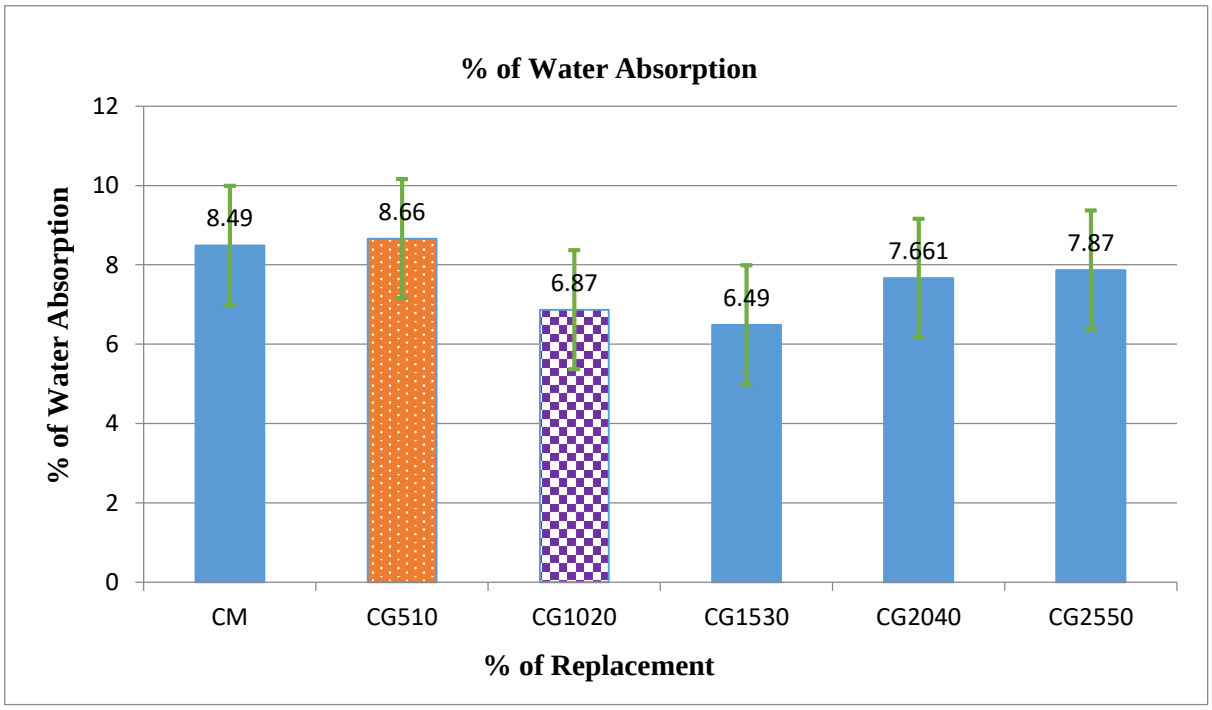

Figure (11): Test results of water absorption

Mortar Triplet Test (Brick Bond Strength)

Investigation in mortar triplet test reflected varied form response after being subjected to the test, as represented in Table 6. CG510 (5% GP, 10% CS) shows a bond strength of 5.25 N/mm², indicating a slight improvement over the control mix. CG1020 (10% GP, 20% CS) exhibits the highest bond strength at 5.54 N/mm² (Figure 12), suggesting that this combination provides optimal bonding properties, potentially due to enhanced pozzolanic activity and improved microstructure. Higher bond strength in the triplet specimen with reference mix suffered brick or substate failure due to greater adhesion strength (Saiz Martinez et al., 2017). CG1530 (15% GP, 30% CS) returns to a bond strength of 5.25 N/mm², indicating that while the performance remains stable, it does not exceed the peak observed in CG1020. The bond strength significantly decreases in CG2040 (20% GP, 40% CS) to 4.14 N/mm² and further in CG2550 (25% GP, 50% CS) to 4.01 N/mm². This reduction suggests that excessive replacement levels may compromise the mortar's bond strength, likely due to increased porosity and reduced cohesive forces. The bond strength or failure load exhibited a decreasing trend with increased GP and CS replacement, potentially due to reduced development length in the pores (Saiz Martinez et al., 2017). The inclusion of glass powder and copper slag in mortar can enhance bond strength, particularly at moderate replacement levels. However, high replacement levels can lead to a decline in bond strength.

Table 6. Responses of specimens toward bond test and their fracture pattern

	At 28 Days	Closely Placed Failed	Separated Sample
A	 0 % Replacement – A1	 0 % Replacement – A2	 0 % Replacement – A3
B	 5/10% Replacement – B1	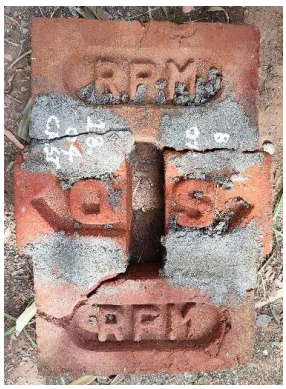 5/10% Replacement – B2	 5/10% Replacement – B3

C	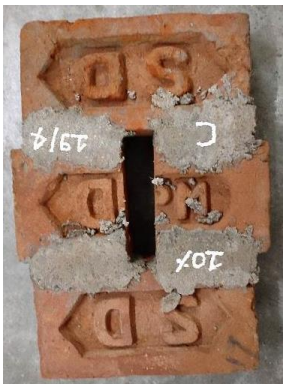 10/20% Replacement – C1	 10/20% Replacement – C2	 10/20% Replacement – C3
D	 15/20% Replacement-D1	 15/20% Replacement-D2	 15/20% Replacement-D3
E	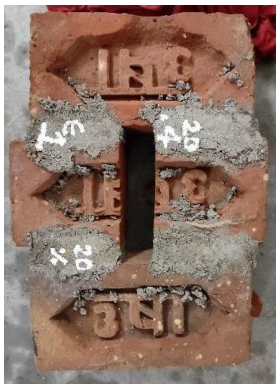 20/40% Replacement-E1	 20/40% Replacement-E2	 20/40% Replacement-E3
F	 25/50% Replacement-F1	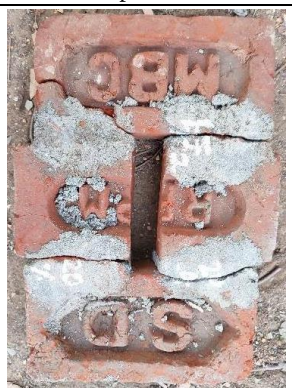 25/50% Replacement-F2	 25/50% Replacement-F3

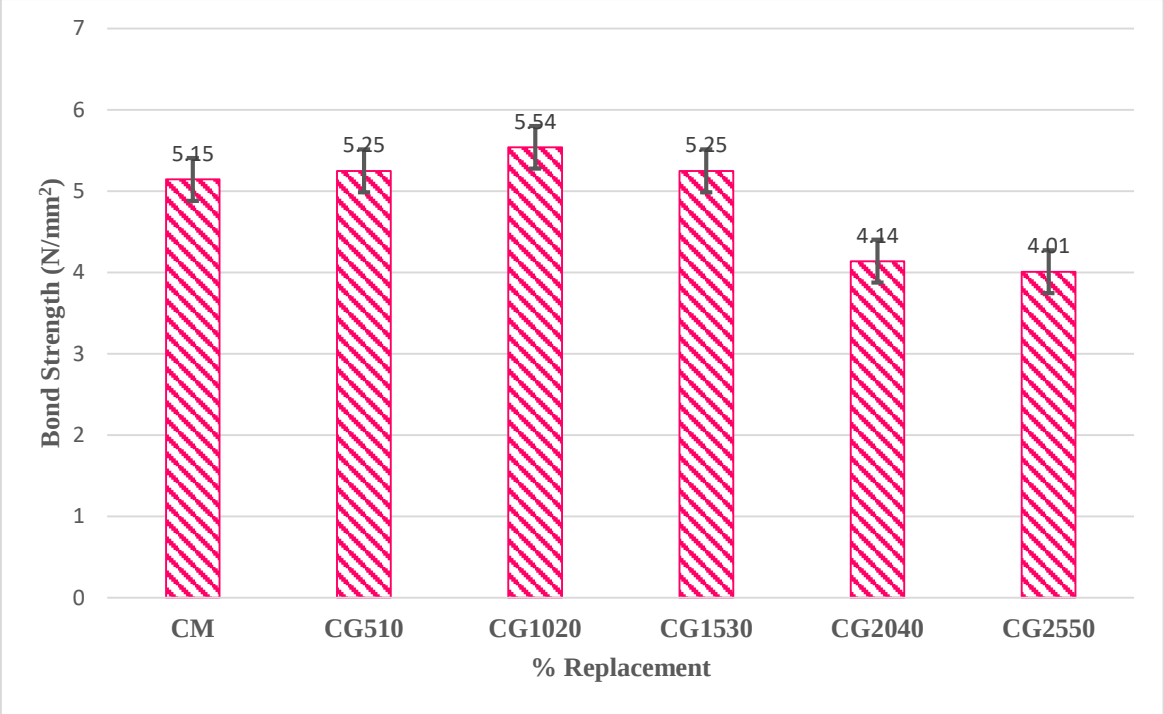

Figure (12): Bond strength of different percentages of replacement

Microstructural Analysis

This study involves the partial replacement of cement and fine aggregate, the primary constituents of mortar, with copper slag. Therefore, it becomes imperative to analyze the microstructure of these blended mortar mixtures. For the microstructural analysis of the control mortar and the various blended mixes, Scanning Electron Microscopy (SEM) and X-ray Diffraction (XRD) were performed to assess their properties and morphology.

SEM Analysis

Scanning Electron Microscopy (SEM) was conducted on a range of mortar specimens to evaluate the compactness of the mortar microstructure resulting from the formation of various hydration products. A representative portion of the hardened concrete or mortar is chosen for analysis. The sample is carefully dried, typically in an oven, to eliminate any moisture that could affect the SEM results. The surface of the sample is then polished for smoothness and coated with a conductive layer, such as gold or carbon, to prevent charge accumulation during imaging. Finally, the prepared sample is secured to an SEM stub with a conductive adhesive for examination. SEM images for the control mortar and the blended mortar are presented in Figure (13). Notably, mortar with CG1020 (10% GP, 20% CS) replacement exhibited a relatively more compact microstructure compared to the control concrete. The finer particle size of these mineral admixtures, in contrast to conventional ones, allows them to fill the pores effectively, contributing to improved packing of the blended mixes containing GP and CS fines. Furthermore, the mortar microstructure becomes denser due to the formation of additional calcium-silicate-hydrate (C-S-H) gel through the secondary hydration of the mineral admixture (Ling et al., 2020).

In Figure 13 (c), larger voids are evident in the mortar microstructure. This is primarily attributed to the higher replacement levels which result in an insufficient amount of calcium required for the formation of C-S-H gel. In the absence of C-S-H gel formation, the fillers lack sufficient bonding between them, ultimately leading to a more porous and weaker mortar (Saiz Martinez et al., 2017).

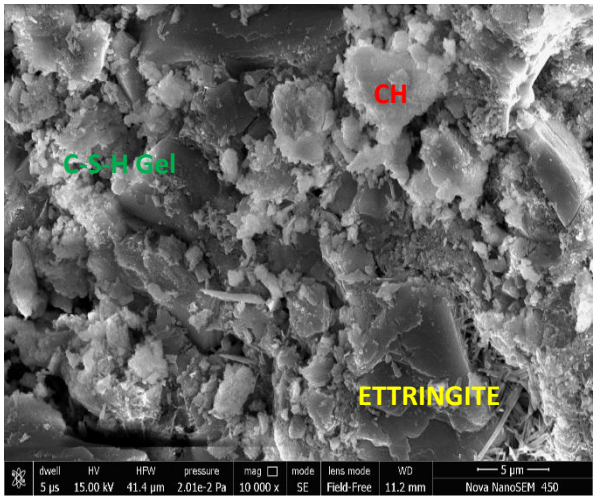

(a) Control mortar

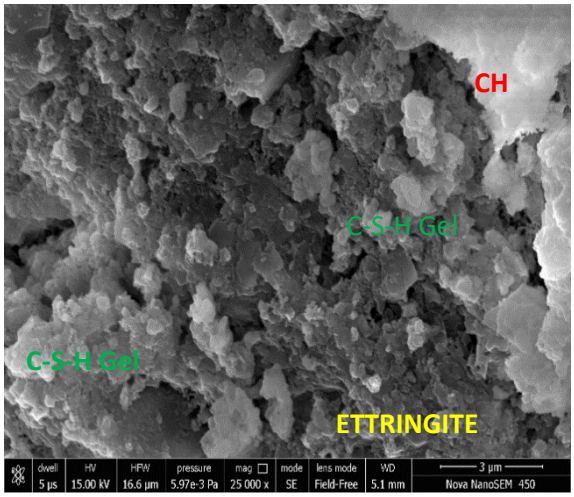

(b) CG1020

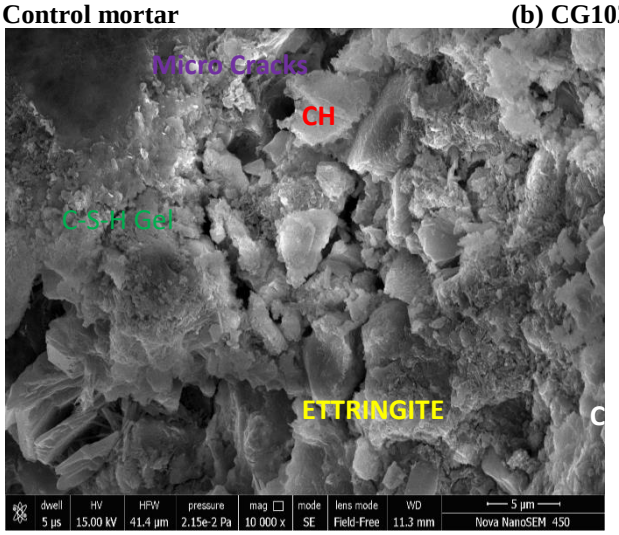

(c) CG2550

Figure (13): Images of SEM analysis

XRD Analysis

The X-ray diffraction (XRD) test determines peak intensities through relative comparisons within the pattern. A suitable portion of the hardened concrete or mortar is chosen for analysis. The sample is carefully ground, often with a mortar and pestle or a mechanical grinder, to achieve a uniform powder. This powder is then sifted through a sieve to ensure consistent particle size, typically under 75 microns. The resulting powder is placed in a sample holder and compacted to create a smooth, even surface for XRD measurement. In Figure (14), higher peaks of calcium hydroxide (CH) were observed between 20 and 40 degrees of two-theta values, indicating the presence of unutilized CH in the control mortar. However, with the introduction of additional silica from GP, this unutilized CH is converted into calcium-silicate-hydrate (C-S-H) (Ling et al., 2020). Figure (14) illustrates the formation of higher peaks of C-S-H between 30 and 80 degrees of two-theta values, accompanied by reduced intensity peaks of CH. These findings are consistent with the results of various mechanical and durability tests, which demonstrate the positive impact of incorporating CS as good fine aggregate and GP as cement.

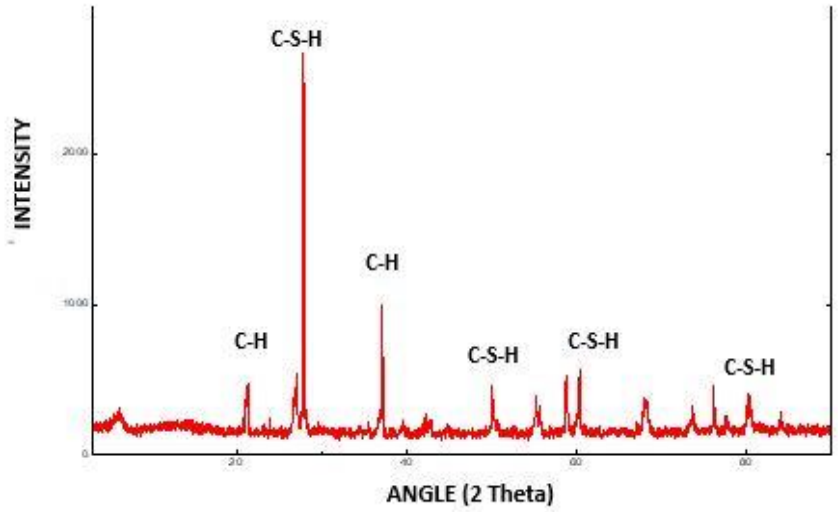

(a) Control mortar

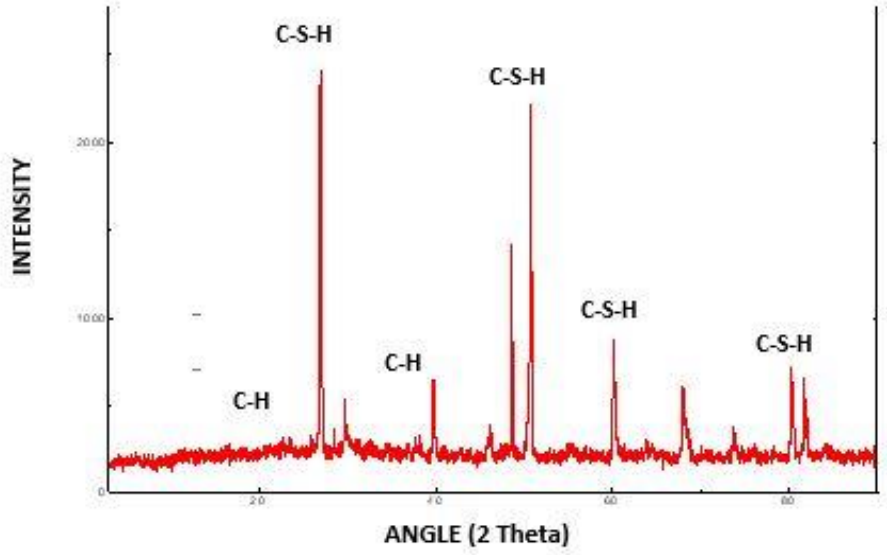

(b) CG1020

Figure (14): Images of XRD analysis

Fourier-transform Infrared Spectroscopy (FTIR) Analysis

For FTIR analysis, a representative portion of hardened concrete or mortar is selected and ground into a fine powder, ensuring uniformity by passing it through a 75-micron sieve. This powdered sample is combined with potassium bromide (KBr) in a specific proportion and compressed into a transparent pellet using a pellet press. The prepared pellet is then analyzed in the FTIR spectrometer to detect functional groups and chemical bonds. The FTIR spectra of the control, CG1020 and CG2550 mixes are presented in Figures (15). The cement hydration process can be identified by the band at approximately 1000 cm^{-1}, observed at 968 cm^{-1} for the control mix, 971 cm^{-1} for the CG1020 mix, and 975 cm^{-1} for the CG2550 mix. The portlandite band is located near 3400 cm^{-1}, with specific values of 3416 cm^{-1}, 3413 cm^{-1}, and 3398 cm^{-1} for the control, CG1020 and CG2550 mixes, respectively. The FTIR spectra indicate slight variations in the hydration of cement clinker and portlandite when CS is used to replace natural fine aggregate.

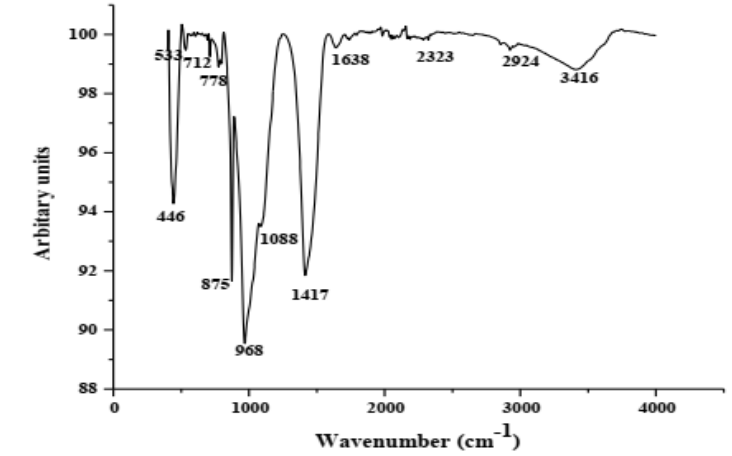

(a) Control

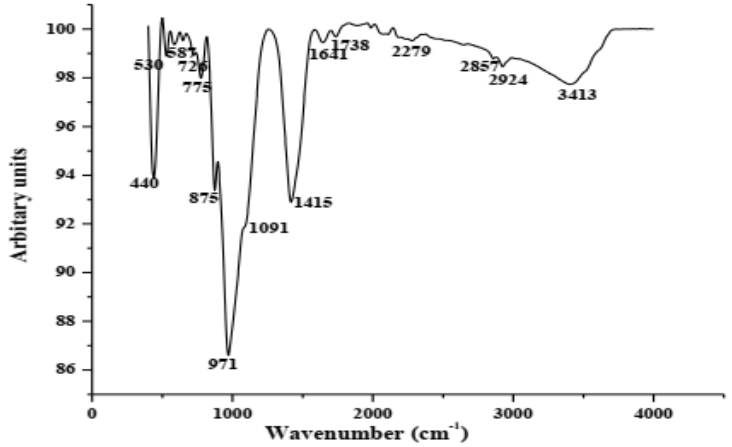

(b) CG1020

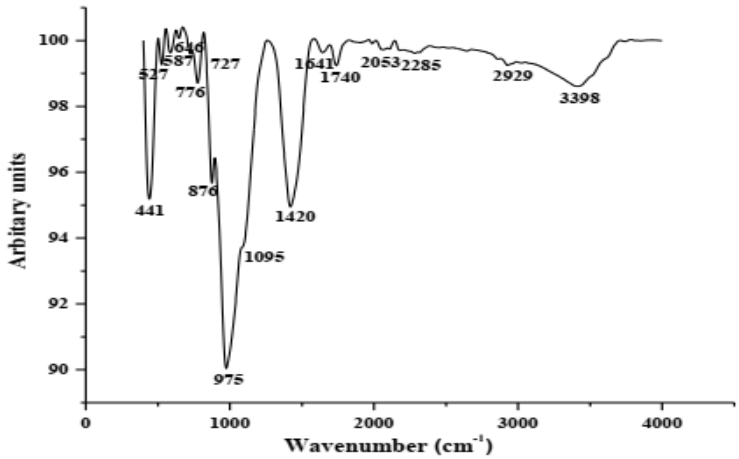

(c) CG2550

Figure (15): FTIR of mortar containing copper slag and glass powder

Thermo-gravimetric Analysis (TGA)

Thermo-gravimetric analysis (TGA) was conducted to assess the impact of increasing temperature at a constant rate. The TGA curves for various mortar mixes are presented in Figure (16). As the temperature increased, a loss in weight was observed. The percentage of weight loss was lowest in mortars prepared with a combination of CS and GP, compared to those made with either CS or GP alone. This behavior is attributed to the reduced availability of portlandite, which reacts with mullite to form calcium-alumino-silicate-hydrate (C-A-S-H). The enhanced hydration observed is

reflected in the improved mechanical properties of mortars containing CS and GP.

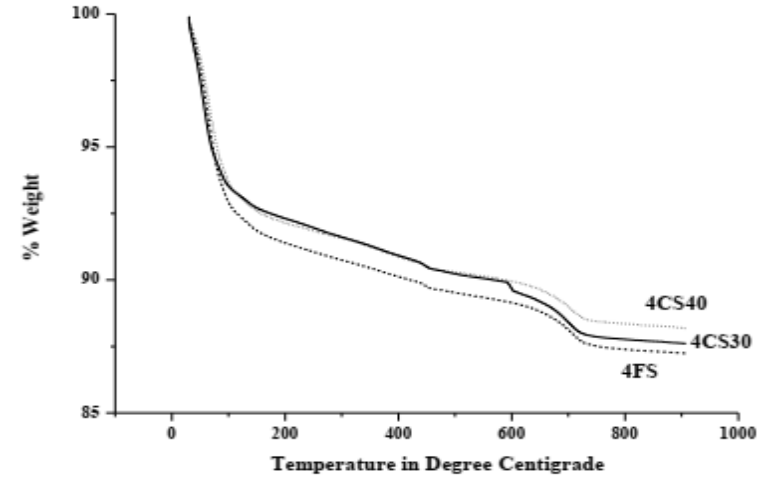

(a) Control mix

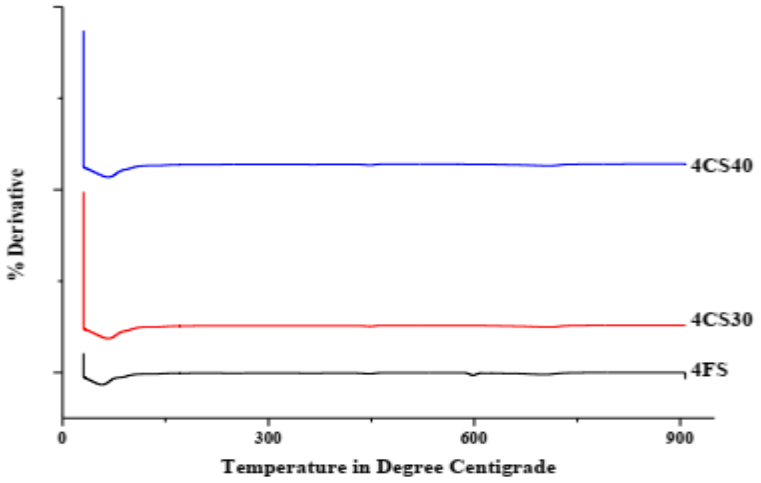

(b) CG1020

Figure (16): DTG curves for control and CG1020% mortar mixes

CONCLUSIONS

This research demonstrates that copper slag with glass powder can be effectively utilized in mortar formulations, with up to a (15% GP, 30% CS) mix replacement, to improve the mechanical performance and environmental sustainability of the resulting mortar. This phrasing better captures the idea of reducing environmental impact without suggesting an enhancement of specific environmental properties. This approach is promising for the sustainable development of construction materials while addressing environmental and waste management concerns related to the copper and glass-producing industry.

- The results affirm that the strategic use of copper slag and glass powder as partial replacements in mortar can lead to improved compressive strength, particularly at moderate replacement levels. Achieving an optimal blend of approximately 10% copper slag and 20% glass powder can provide enhanced mechanical properties while simultaneously contributing to sustainable construction practices. However, to maximize the benefits of these materials, it is crucial to avoid exceeding these replacement thresholds, as doing so may lead to reduced strength and durability.
- The replacement of traditional materials with GP and CS appears to have beneficial effects on water absorption up to a certain level. The optimal ranges seem to be around 10% GP and 20% CS, where water absorption is minimized. The increasing trend in water absorption at higher replacement levels

indicates potential limitations of these materials when used in excess.

- The inclusion of glass powder and copper slag in mortar can enhance bond strength, particularly at moderate replacement levels. However, high replacement levels can lead to a decline in bond strength, indicating that careful selection of replacement percentages is crucial for optimizing the performance of mortar.
- The positive results observed in the mechanical and durability properties of the blended mortar mixes were validated through comprehensive microstructural analysis. Techniques, such as Scanning Electron Microscopy (SEM), X-ray Diffraction (XRD), Fourier Transform Infrared Spectroscopy (FTIR), and Thermo-gravimetric Analysis (TGA), were employed to examine mortar mixes containing varying proportions of copper slag and glass powder. The findings indicated a denser microstructure, which can be primarily attributed to the increased content of fine particles and the formation of secondary calcium-silicate-hydrate (C-S-H) gel. This enhanced microstructural integrity contributes significantly to the improved performance of the blended mortars, supporting their potential application in sustainable construction practices.

In conclusion, this study demonstrates that incorporating copper slag and glass powder into mortar formulations at replacement levels of up to 15% glass powder and 30% copper slag can lead to significant enhancements in both mechanical and environmental properties. This strategic use of industrial by-products not only improves the performance of the mortar, but also supports sustainable construction practices and effective waste management in the glass and copper industries. By utilizing these materials, the construction sector can reduce its environmental footprint while simultaneously enhancing the quality and durability of building materials.

Acknowledgements

This work was supported by Swami Keshvanand Institute of Technology (SKIT), Jaipur, Malviya National Institute of Technology, Jaipur, and Arya Institute of Engineering & Technology. The authors sincerely acknowledge the facilities provided by SKIT & MNIT for carrying out the research work. The authors also acknowledge the support of all civil engineering lab and teaching staff.

REFERENCES

Abukersh, S.A., and Fairfield, C.A. (2011). "Recycled aggregate concrete produced with red-granite dust as a partial cement replacement". Construction and Building Materials, 25 (10), 4088-4094. https://doi.org/10.1016/j.conbuildmat.2011.04.047

Al-Jabri, K.S., Al-Harthi, M.A., and Al-Saidy, A.H. (2006). "Effect of copper slag as a fine aggregate on cement mortars and concrete properties". Construction and Building Materials, 20 (8), 578-585. 5https://doi.org/10.1016/j.conbuildmat.2005.02.005

Aouan, B., Alehyen, S., Fadil, M., El Alouani, M., Khabbazi, A., Atbir, A., and Taibi, M. (2021). "Compressive strength optimization of metakaolin-based geopolymer by central composite design". Chemical Data Collections, 31, 100636, https://doi.org/10.1016/j.cdc.2020.100636

ASTM C109M-16a. "Standard test method for compressive strength of hydraulic cement mortar (using 2-inch or 50-mm cube specimen)".

ASTM C1148-92a. "Standard test method for measuring the drying shrinkage of masonry mortar".

ASTM C1437-15. "Standard test method for flow of hydraulic cement mortar".

ASTM C642-13. "Standard test method for density, absorption, and void in hardened concrete".

Babu, T., and Thangaraj, S. (2023). "A novel approach for the synthesis of eco-friendly geopolymer ternary blended mortar with GGBS, sugarcane bagasse ash, and sewage sludge ash under ambient curing conditions". KSCE J. Civ. Eng., 27, 3441-3454. https://doi.org/10.1007/S12205-023-1842-X/METRICS

Batis, G., Pantazopoulou, P., Tsivilis, S., and Badogiannis, E. (2005). "The effect of metakaolin on the corrosion behavior of cement mortars". Cement and Concrete Composites, 27 (1), 125-130.

Bilir, T., Gencel, O., and Topcu, I.B. (2015). "Properties of mortars with fly ash as fine aggregate." Construction and Building Materials, 93, 782-789. 1https://doi.org/10.1016/j. conbuildmat.2015.05.021

Borhan, M.M., and Mohamed, S.N. (2022). "Laboratory study of water absorption of modified mortar".

BS 1015-12. (2000). "Methods of test for mortar for masonry: Determination of adhesive strength of hardened rendering and plastering mortar on substrates".

Casagrande, C.A. (2023). "Copper slag in cementitious composites: A systematic review" Journal of Building Engineering, 78, 10725. https://doi.org/10.1016/j.jobe.2023.107725

Christy, C.F., and Tensing, D. (2010). "Effect of class-F fly ash as a partial replacement with cement and fine aggregate in mortar." Indian Journal of Engineering and Materials Sciences, 17, 140-144.

Deb, P.S., Nath, P., and Sarker, P.K. (2015). "Drying shrinkage of slag blended fly ash geopolymer concrete cured at room temperature". Procedia Eng., 125, 594-600. https://doi.org/10.1016/J.PROENG.2015.11.066

Degirmenci, N., and Yilmaz, A. (2011). "Use of pumice fine aggregate as an alternative to standard fine aggregate in the production of lightweight cement mortar". Indian Journal of Engineering and Material Science, 18, 61-68.

Driouich, A. Chajri, F., El Hassani, S.E.A., Britel, O., Belouafa, S., Khabbazi, A., and Chaair, H. (2020). "Optimization synthesis of geopolymer-based mixture metakaolin and fly ash activated by alkaline solution". J. Non-Cryst. Solids, 544120197. https://doi.org/10.1016/j. jnoncrysol.2020.120197

Duan, P., Yan, C., Luo, W., and Zhou, W. (2016). "Effects of adding nano-TiO2 on compressive strength, drying shrinkage, carbonation and microstructure of fluidized bed fly ash based geopolymer paste". Construct. Build. Mater., 106, 115-125, https://doi.org/10.1016/j.conbuildmat.2015.12.095

Fan, J., Yan, J., Zhou, M., Xu, Y., Lu, Y., Duan, P., Zhu, Y., Zhang, Z., Li, W., Wang, A., and Sun, D. (2023). "Heavy metal immobilization of ternary geopolymer based on nickel slag, lithium slag and metakaolin". J. Hazard Mater, 453131380. https://doi.org/10.1016/J.JHAZMAT.2023.131380

Gupta, L.K., and Vyas, A.K. (2018). "Impact on mechanical properties of cement fine aggregate mortar containing waste granite powder".

Hwang, K.R., and Noguchi, T. (1998). "Effect of fine aggregate replacement on the rheology, compressive strength, and carbonation properties of fly ash mortar." ACI Special Publication SP-178, 401-410.

Irki, I., Debieb, F., Quzadid, S., Larouci, H., Settari, C., and Boukhelkhel, D. (2023). "Effect of blaine fineness of recycling brick powder replacing cementitious materials in self-compacting mortar".

IS 2386-1963 Part-3. (1963). "Method of physical testing for aggregates for concrete: Specific gravity, density, voids, absorption, and bulking".

IS 2720-1980 Part-3. (1980). "Methods of soil for soils: Determination of specific gravity. Section 1: Fine grained soil".

IS 383-2016. (2016). "Natural coarse and fine aggregates for concrete & mortar".

IS 4031-2019 Part-1. (2019). "Methods of physical testing for hydraulic cement: Determination of fineness by dry sieving".

IS 4031-2019 Part-3. (2019). "Method of physical testing for hydraulic cement: Determination of soundness".

IS 4031-2019 Part-4. (2019). "Methods of physical testing for hydraulic cement: Determination of consistency of standard cement paste".

IS 4031-2019 Part-5. (2019). "Methods of physical tests for hydraulic cement".

IS Code 4031-1988 Part-10. (1988). "Methods of physical tests for hydraulic cement: Determination of drying shrinkage".

IS Code 4031-1988 Part-3: Method of physical tests for hydraulic cement: Determination of soundness

IS Code 4031-1998 Part-7. (1998). "Methods of physical tests for hydraulic cement: Determination of compressive strength of masonry cement".

Jain, K.L., Sharma, D.K., Choudhary, R., and Bhargava, S. (2022). "Impact of waste iron slag on mechanical and durability properties of concrete". Jordan Journal of Civil Engineering, 17 (1).

Jumaa, N.H., Ali, I.M., Nasr, M.S., and Falah, M.W. (2022). "Strength and microstructural properties of binary and ternary blends in fly ash-based geopolymer concrete". Case Stud. Constr. Mater., 17e01317. https://doi.org/10.1016/j.cscm.2022.e01317

Kallel, T., Kallel, A., and Samet, B. (2021). "Durability of mortar made with fine aggregate wash".

Kou, S.C., and Poon, C.S. (2020). "Effect of different kinds of recycled aggregate on properties of rendering mortar".

Lalit, K.G., and Ashok, K.V. (2021). "Impact on mechanical properties of cement fine aggregate mortar containing waste granite powder".

Ling, T.C., and Poon, C.S. (2020). "Effect of particle size of treated CRT funnel glass on properties of cement mortar".

Mobasher, B., Devaguptapu, R., and Arino, A.M. (1996). "Effect of copper slag on the hydration of blended cementitious mixtures". In: Proceedings of ASCE Materials Engineering Conference—Materials for the New Millennium. Washington, DC, November 10-14.

Ramadoss, P., and Sundararajan, T. (2014). "Utilization of lignite-based bottom ash as partial replacement of fine aggregate in masonry mortar". Arabian Journal for Science and Engineering, 39, 737-745.

Rivera, P., and Nazor, T. (2013). "Use of copper slag as fine aggregate and partial cement replacement".

Saiz Martinez, P., Gonzalez Cortina, M., Fernandez, F., and Rodriguez Sanchez, A. (2017). "Comparative study of three types of fine recycled aggregates from construction and demolition waste and their use in masonry fabrication."

Saranya, P., Nagarajan, P., and Shashikala, A.P. (2021). "Engineering and durability properties of slag-dolomite geopolymer mortars". Proceedings of the Institution of Civil Engineers: Construction Materials. https://doi.org/10.1680/jcoma.18.00096

Sivasakthi, M., Jeyalakshmi, R., and Rajamane, N.P. (2021). "Fly ash geopolymer mortar: Impact of the substitution of river sand by copper slag as a fine aggregate on its thermal resistance properties". J. Clean. Prod., 279, 123766. https://doi.org/10.1016/j.jclepro.2020.123766

Soriano, L., Monzó, J., Bonilla, M., Tashima, M.M., Payá, J., and Borrachero, M.V. (2013). "Effect of pozzolans on the hydration process of Portland cement cured at low temperatures". Cement and Concrete Composites, 42, 41-48.

Sreenivasulu, C., Jawahar, J.G., and Sashidhar, C. (2020). "Effect of copper slag on micro, macro, and flexural characteristics of geopolymer concrete". J. Mater. Civ. Eng., 32, 04020086. https://doi.org/10.1061/(ASCE)MT.1943-5533.0003157

Srinivasreddy, K., Bala Murugan, S., Jindal, B.B., and Vali, K.S. (2022). "Experimental study on the properties of ternary blended geopolymer rich mortar". Innovative Infrastructure Solutions, 7, 1-9. https://doi.org/10.1007/S41062-022-00757-4/METRICS

Swanepoel, C.A.S.J.C. (2002). "Utilization of fly ash in a geopolymeric material". Appl. Geochem., 17, 1143-1148, https://doi.org/10.1016/S0883-2927(02) 00005-7

Tironi, A., Trezza, M.A., Irassar, E.F., and Scian, A.N. (2012). "Thermal treatment of kaolin: Effect on the pozzolanic activity". Procedia-Materials Science, 1, 343-350. https://doi.org/10.1016/j.mspro.2012.06.046

Topçu, L.B., and Bilir, T. (2010). "Effect of bottom ash as fine aggregate on shrinkage cracking of mortars". ACI Materials Journal, 107 (M08), 48-56.

Xu, Z., Yue, J., Pang, G., Li, R., Zhang, P., and Xu, S. (2021). "Influence of the activator concentration and solid/liquid ratio on the strength and shrinkage characteristics of alkali-activated slag geopolymer pastes". Adv. Civ. Eng., 2021. https://doi.org/10.1155/2021/6631316

Yuma Saeki, K.N.D.K. Kazunori Fujikake, and Tatsuya Sasatani. (2022). "Development of cast-in-place FA-GGBFS-based geopolymer mortar: An experimental study". Pract. Period. Struct. Des. Construct., 27, 1-8, https://doi.org/10.1061/(ASCE)SC.1943-5576.0000681